J|A|C|S ARTICLES

Published on Web 11/15/2010

Activation of Methane by Zinc: Gas-Phase Synthesis, Structure, and Bonding of $HZnCH_3$

Michael A. Flory,[†] Aldo J. Apponi,[‡] Lindsay N. Zack, and Lucy M. Ziurys*

Department of Chemistry, Department of Astronomy, and Steward Observatory, University of Arizona, 933 North Cherry Avenue, Tucson, Arizona 85721, United States

Received July 10, 2010; E-mail: lziurys@email.arizona.edu

Abstract: The methylzinc hydride molecule, $HZnCH_3$, has been observed in the gas phase for the first time in the monomeric form using high-resolution spectroscopic techniques. The molecule was synthesized by two methods: the reaction of dimethylzinc with hydrogen gas and methane in an AC discharge and the reaction of zinc vapor produced in a Broida-type oven with methane in a DC discharge. $HZnCH_3$ was identified on the basis of its pure rotational spectrum, which was recorded using millimeter/submillimeter direct-absorption and Fourier transform microwave techniques over the frequency ranges 332−516 GHz and 18−41 GHz, respectively. Multiple rotational transitions were measured for this molecule in seven isotopic variants. *K*-ladder structure was clearly present in all of the spectra, indicating a molecule with C_{3v} symmetry and a $^1A_1$ ground electronic state. Extensive quadrupole hyperfine structure arising from the ^{67}Zn nucleus was observed for the $H^{67}ZnCH_3$ species, suggesting covalent bonding to the zinc atom. From the multiple isotopic substitutions, a precise structure for $HZnCH_3$ has been determined. The influence of the axial hydrogen atom slightly distorts the methyl group but stabilizes the Zn−C bond. This study suggests that $HZnCH_3$ can be formed through the oxidative addition of zinc to methane in the gas phase under certain conditions. $HZnCH_3$ is the first metal−methane insertion complex to be structurally characterized.

Introduction

The interaction between metal atoms and small alkanes is important in many areas of chemistry. Because of their stability, alkanes are generally abundant and useful as raw materials, but they can be quite inert.[1] However, the reaction of a hydrocarbon compound at a metal center can lead to the activation of the C−C and C−H bonds, thereby increasing the utility of such compounds. In fact, the metal activation process has many known applications in catalysis,[2−5] biochemistry,[6] and organic synthesis.[7−9] The 3d metals are particularly relevant in this context. Thus, considerable research over the past few decades has been devoted to elucidating the mechanisms by which this activation can occur.[10,11]

One mechanism that has received considerable attention is the insertion of transition-metal atoms into the simplest C−H bonds, namely, those of methane. There have been numerous experimental studies of this process over several decades. Margrave and co-workers used IR spectroscopy to demonstrate that the 3d metals Mn through Zn insert into CH_4 in a 15 K matrix upon irradiation with UV light.[12−15] Other studies showed that the 3d metals Sc, Ti, V, and Cr undergo this oxidative addition reaction with methane in argon matrices upon metal photoexcitation.[16−20] These matrix experiments revealed that methylmetal hydrides, $HMCH_3$ (M = metal), are stable products in solid-phase reactions. Gas-phase studies of methane bond activation by metals have been limited to molecular beam experiments involving excited metal atoms or ions reacting with CH_4 or larger hydrocarbons, in which reaction energies and cross sections have been measured.[21−23] Breckenridge and Renlund,

[†] Present address: CNA, Alexandria, VA 22311.
[‡] Present address: Geost Inc., Tucson, Arizona 85741.

(1) Iverson, C. N.; Carter, C. A. G.; Scollard, J. D.; Pribisko, M. A.; John, K. D.; Scott, B. L.; Baker, R. T.; Bercaw, J. E.; Labinger, J. A. *ACS Symp. Ser.* **2004**, *885*, 319–333.
(2) Ceyer, S. T. *Science* **1990**, *249*, 133–139.
(3) Böhme, D. K.; Schwarz, H. *Angew. Chem., Int. Ed.* **2005**, *44*, 2336–2354.
(4) Schröder, D.; Schwarz, H. *Angew. Chem., Int. Ed. Engl.* **1995**, *34*, 1973–1995.
(5) Roithová, J.; Schröder, D. *Chem. Rev.* **2010**, *110*, 1170–1211.
(6) Zhang, D.; Wang, R.; Zhu, R. *Aust. J. Chem.* **2005**, *58*, 82–85.
(7) Breckenridge, W. H. *J. Phys. Chem.* **1996**, *100*, 14840–14855.
(8) Armentrout, P. B. *Top. Organomet. Chem.* **1999**, *4*, 1–45.
(9) Armentrout, P. B. *Int. J. Mass Spectrom.* **2003**, *227*, 289–302.
(10) Blomberg, M. R. A.; Siegbahn, P. E. M.; Nagashima, U.; Wennerberg, J. *J. Am. Chem. Soc.* **1991**, *113*, 424–433.
(11) Schwarz, H.; Schröder, D. *Pure Appl. Chem.* **2000**, *72*, 2319–2332.
(12) Billups, W. E.; Konarski, M. M.; Hauge, R. H.; Margrave, J. L. *J. Am. Chem. Soc.* **1980**, *102*, 7393–7394.
(13) Billups, W. E.; Chang, S.-C.; Hauge, R. H.; Margrave, J. L. *J. Am. Chem. Soc.* **1995**, *117*, 1387–1392.
(14) Kafafi, Z. H.; Hauge, R. H.; Margrave, J. L. *J. Am. Chem. Soc.* **1985**, *107*, 6134–6135.
(15) Chang, S.-C.; Hauge, R. H.; Billups, W. E.; Margrave, J. L.; Kafafi, Z. H. *Inorg. Chem.* **1988**, *27*, 205–206.
(16) Andrews, L.; Cho, H.-G.; Wang, X. *Inorg. Chem.* **2005**, *44*, 4834–4842.
(17) Cho, H.-G.; Andrews, L.; Marsden, C. *Inorg. Chem.* **2005**, *44*, 7634–7643.
(18) Cho, H.-G.; Andrews, L. *J. Phys. Chem. A* **2006**, *110*, 3886–3902.
(19) Cho, H.-G.; Andrews, L. *Organometallics* **2007**, *26*, 633–643.
(20) Greene, T. M.; Andrews, L.; Downs, A. J. *J. Am. Chem. Soc.* **1995**, *117*, 8180–8187.
(21) Breckenridge, W. H.; Renlund, A. M. *J. Phys. Chem.* **1978**, *82*, 1474–1484.
(22) Breckenridge, W. H.; Renlund, A. M. *J. Phys. Chem.* **1979**, *83*, 1145–1150.
(23) Georgiadis, R.; Armentrout, P. B. *J. Am. Chem. Soc.* **1986**, *108*, 2119–2126.

10.1021/ja106121v

for example, determined that the cross sections for the quenching of excited Cd, Hg, and Zn atoms by CH_4 were generally small.[21,22] In contrast to the solid-phase work, $HMCH_3$ compounds in the gas phase are expected to be unstable intermediates of metal insertion reactions, leading to the formation of MH and the CH_3 radical.[24]

The insertion of metal atoms into methane has also been the focus of theoretical investigations. Many of the proposed insertion pathways involve metal atoms in excited electronic states, consistent with experimental evidence. However, there is some disagreement about the identity of these excited states.[24] For example, the insertion of Zn, Cd, or Hg into methane is thought to occur through the ^{3}P excited state; however, this reaction could occur via the ^{1}P state as well.[24,25] Copper is thought to add to CH_4 in its ^{2}P excited state,[26] but the ^{2}D state could also participate. Oxidative additions of metals to CH_4 and larger hydrocarbons have also been explained in terms of spin uncoupling of the electrons in the C−H bond and the metal, which lowers the reaction activation energy.[27] More recent calculations have suggested that while both Pd and Be form stable $HMCH_3$ molecules upon insertion into methane, Zn, Cd, Mg, and Ca do not.[28] The $HMCH_3$ species take on a variety of structures as well. Some, such as $HFeCH_3$, have linear C−M−H backbones, giving rise to C_{3v} geometries;[29] however, both the Pd and Ca species are expected to be bent, with C−M−H bond angles of 87.2 and 129.2°, respectively.[28]

In order to further explore the oxidative addition of metals to methane, we synthesized $HZnCH_3$ in the gas phase; examined its structure, relative stability, and bonding properties; and investigated its formation by the reaction of Zn atoms with CH_4. The molecule was created in monomeric form by the reaction of Zn vapor with CH_4 as well as from the precursors $Zn(CH_3)_2$ and H_2. Two high-resolution spectroscopic methods were used to characterize $HZnCH_3$ and record its rotational spectrum. Observations on $H^{64}ZnCH_3$ and six other isotopologues have established an unambiguous identification of this molecule and enabled a precise determination of its structure. The strong signals exhibited by $HZnCH_3$ suggest that it is relatively stable at elevated temperatures. In this report, we present our results and discuss possible mechanisms for the gas-phase formation of this species.

Experimental Section

The $HZnCH_3$ molecule was characterized in the gas phase using techniques of high-resolution rotational spectroscopy. A combination of millimeter/submillimeter direct-absorption and Fourier transform microwave (FTMW) methods were used to record the spectrum of this species across a wide frequency range. The FTMW technique also offers extremely high resolution (2 kHz at 4−40 GHz), enabling a detailed examination of small spectroscopic splittings arising from interactions of nuclear spins. The experimental work was done in a series of investigations. First, $HZnCH_3$ was identified in the gas phase on the basis of its rotational spectrum using millimeter/submillimeter direct-absorption measurements. Spectra of several isotopically substituted species were also measured to confirm the identification. Second, additional spectra were recorded at lower frequencies using FTMW methods to examine hyperfine structure arising from the ^{67}Zn nucleus and provide additional structural information. From the complete data set, the rotational constants for each isotopologue and consequently the moments of inertia were determined. From these data, the geometry was calculated. Finally, the spectroscopic signatures of $HZnCH_3$ were used to examine possible synthetic routes.

Spectrometers. The millimeter-wave measurements (332−516 GHz) were obtained using the velocity-modulation instrument in the Ziurys lab, which is described in detail elsewhere.[30] Briefly, the spectrometer consists of a tunable, coherent source of millimeter/submillimeter radiation, a sealed glass reaction cell, and a detector. The radiation sources are Gunn oscillator/varacter multiplier combinations, which span a range of 65−850 GHz; the source is phase-locked to a stable frequency reference. The reaction cell is continuously evacuated to ∼1 mTorr using a Roots blower system, and it is chilled to −65° using methanol. The chamber also contains two ring electrodes that create a longitudinal AC discharge. The detector is a helium-cooled InSb hot-electron bolometer. The species of interest is synthesized in the cell while the source is scanned in frequency and the radiation focused through the chamber and into the detector. When the frequency is resonant with a molecular transition, an absorption signal is measured. Phase-sensitive detection at 2*f* is carried out by FM modulation of the Gunn oscillator. The resolution of the instrument is ±50 kHz.

Additional chemical experiments were conducted using the high-temperature direct-absorption spectrometer belonging to the Ziurys group.[31] This instrument is similar to the one described above, but the optics are more complex because the radiation beam is passed through the reaction chamber twice. The cell also contains a Broida-type oven used for metal vaporization (see ref 32).

Spectral measurements were conducted over the range 18−37 GHz using the Balle−Flygare-type[33] pulsed FTMW spectrometer in the Ziurys lab. In this case, the reactant gases are introduced into a Fabry−Perot cavity using a pulsed solenoid valve set at a 40° angle relative to the optical axis. The cavity is a large steel chamber under low (10^{-8} Torr) vacuum. The expansion uses a stagnation pressure of 40 psi behind a 0.8 mm nozzle orifice and a 10 Hz repetition rate. Ring electrodes are attached to the end of the nozzle, producing a DC discharge that is passed through the exiting gas. Immediately after the reactant mixture leaves the nozzle/discharge source, a pulse of microwaves with a given frequency and bandwidth (∼300 kHz) is sent into the chamber. If the molecules created in the gas flow are resonant with a frequency in the microwave pulse, they will absorb the radiation and then emit at those frequencies a short time later. These emission signals are recorded as a function of time, generating the so-called "free-induction decay" (FID). The Fourier transform of the FID produces a spectrum. The spectra are recorded as Doppler doublets with a full-width at half-maximum of 5 kHz per feature. Further details about the instrument can be found in ref 34.

Gas-Phase Synthesis. Initially, methylzinc hydride was synthesized in the gas phase directly from dimethylzinc (97% Alfa Aesar) in a 300 W AC discharge in argon inside the millimeter/submillimeter spectrometer glass reaction chamber. A mixture of approximately 2 mTorr $Zn(CH_3)_2$ and 20 mTorr Ar produced observable spectral signals, which were subsequently optimized with the addition of 5 mTorr CH_4 and 10 mTorr H_2. A pale-blue glow, likely arising from atomic zinc, was evident in the discharge during the creation of $HZnCH_3$. Isotopic substitutions were carried out using $^{13}CH_4$ and D_2 for $HZn^{13}CH_3$ and $DZnCH_3$, respectively. The

(24) Alikhani, M. E. *Chem. Phys. Lett.* **1999**, *313*, 608–616.
(25) Castillo, S.; Ramírez-Solís, S.; Díaz, D.; Poulain, E.; Novaro, O. *Mol. Phys.* **1994**, *81*, 825–836.
(26) Poirier, R. A.; Ozin, G. A.; McIntosh, D. F.; Csizmadia, I. G.; Daudel, R. *Chem. Phys. Lett.* **1983**, *101*, 221–228.
(27) Minaev, B. F.; Ågren, H. *Adv. Quantum Chem.* **2001**, *40*, 191–211.
(28) de Jong, G. T.; Visser, R.; Bickelhaupt, F. M. *J. Organomet. Chem.* **2006**, *691*, 4341–4349.
(29) Granucci, G.; Persico, M. *THEOCHEM* **1993**, *283*, 111–116.
(30) Savage, C.; Ziurys, L. M. *Rev. Sci. Instrum.* **2005**, *76*, 043106.
(31) Ziurys, L. M.; Barclay, W. L., Jr.; Anderson, M. A.; Fletcher, D. A.; Lamb, J. W. *Rev. Sci. Instrum.* **1994**, *65*, 1517–1522.
(32) Allen, M. D.; Ziurys, L. M.; Brown, J. M. *Chem. Phys. Lett.* **1996**, *257*, 130–136.
(33) Balle, T. J.; Flygare, W. *Rev. Sci. Instrum.* **1981**, *52*, 33–45.
(34) Sun, M.; Apponi, A. J.; Ziurys, L. M. *J. Chem. Phys.* **2009**, *130*, 034309.

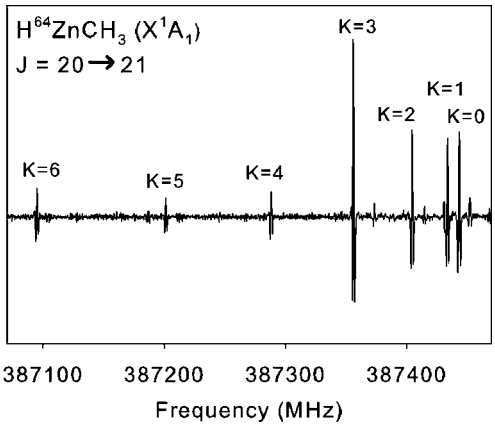

Figure 1. Spectrum of the $J = 20 \rightarrow 21$ rotational transition of $H^{64}ZnCH_3$, measured with the velocity-modulation spectrometer near 387 GHz. The $K = 0-6$ components exhibit the classic prolate-symmetric-top pattern, and spin statistics cause the increase in the intensity of the $K = 3$ feature. The spectrum is a composite of four scans, each 100 MHz in spectral width and acquired in 60 s.

zinc isotopologues were measured in natural abundance ($^{64}Zn/^{66}Zn/^{67}Zn/^{68}Zn = 49:28:4:19$).

In the FTMW experiments, a gas sample was prepared by diluting $Zn(CH_3)_2$ to 0.2% in argon in an evacuated 30 L gas cylinder and pressurizing the container to 200 psi (absolute). This mixture was then introduced into the spectrometer cell through the pulsed discharge nozzle. The DC discharge was run at a voltage of 1 kV with a current of ~50 mA to create $HZnCH_3$. This method was used to record the spectra of the three zinc isotopologues $H^{64}ZnCH_3$, $H^{66}ZnCH_3$, and $H^{67}ZnCH_3$ in natural abundance as well as the spectra of the ^{13}C-substituted species.

In order to investigate the insertion of zinc atoms into methane, an alternate synthesis of $HZnCH_3$ was attempted in the high-temperature system. In this case, pure zinc metal (99.9%, Aldrich) was vaporized in a Broida-type oven and then reacted with a mixture of CH_4 (10 mTorr) and argon (30 mTorr) in a flow reaction chamber. A DC discharge (500 V, 0.3 A) was used to facilitate the synthesis. This approach successfully produced spectral signals of $HZnCH_3$. These signals were not present without the DC discharge.

Results

Identifying the Gas-Phase Spectra. The $HZnCH_3$ molecule was identified in the $Zn(CH_3)_2$/Ar mixture after scanning the 382−412 GHz region continuously in frequency in 100 MHz increments with the velocity-modulation spectrometer. Four very similar spectral patterns, each characteristic of a molecule with C_{3v} symmetry (i.e., a "symmetric top"), were observed. The four patterns had a relative intensity ratio matching that of the four zinc isotopes ^{64}Zn, ^{66}Zn, ^{67}Zn, and ^{68}Zn. Doublet splittings were not apparent in these patterns, indicating that they did not arise from the $ZnCH_3$ radical, which has a doublet ground electronic state (X^2A_1). The closed-shell $ZnCH_3^+$ cation was also ruled out by employing velocity modulation,[30] which selectively eliminates spectra of neutral molecules. Removal of $Zn(CH_3)_2$ from the reaction chamber caused the immediate disappearance of the spectral features. Finally, addition of H_2 caused the spectral intensity to increase 3-fold. Such evidence suggested that the origin of the molecular signals was $HZnCH_3$. Isotopic substitutions of D and ^{13}C produced $DZnCH_3$ and $HZn^{13}CH_3$, respectively, at the frequencies predicted for the given changes in mass, confirming the identification of $HZnCH_3$. A typical spectral signal for $HZnCH_3$ is shown in Figure 1.

The spectral pattern shown in Figure 1 is distinct to a prolate symmetric top, a species with C_{3v} symmetry and two unique moments of inertia, labeled I_a and I_b. For this type of molecule, the rotational energy levels follow the formula[35]

$$F(J,K) = BJ(J+1) - D_J[J(J+1)]^2 + (A-B)K^2 - D_{JK}J(J+1)K^2 \quad (1)$$

where J is the rotational quantum number; K is the quantum number for the projection of the rotational angular momentum vector **J** along the C_{3v} symmetry axis; A and B are the rotational constants, which are related directly to the moments of inertia I_a and I_b, respectively; and D_J and D_{JK} are fourth-order centrifugal distortion terms. Higher-order centrifugal distortion constants are usually necessary to fully characterize a spectrum. By definition, $J = 0, 1, 2, 3, \ldots$ and $K \leq J$, giving rise to a series of energy levels often termed "K-ladder" structure (i.e., for $J = 0$, $K = 0$; for $J = 1$, $K = 1$ and 0; for $J = 2$, $K = 0$, 1, and 2; etc.). Each rotational transition ($J \rightarrow J + 1$) follows the strong electric dipole selection rules $\Delta J = \pm 1$ and $\Delta K = 0$. Therefore, a symmetric-top spectral pattern is immediately recognizable by the presence of K components having a relative frequency spacing of 1:3:5:7:... starting with $K = 0$. Figure 1 shows this classic pattern for the $J = 20 \rightarrow 21$ transition of $H^{64}ZnCH_3$. Because spin statistics apply for the three equivalent methyl protons, the $K = 3n$ (ortho) components have twice the intensity of the $K \neq 3n$ (para) components.[35] Nearly identical spectral patterns were observed for $H^{66}ZnCH_3$, $H^{68}ZnCH_3$, $DZnCH_3$, and $H^{64}Zn^{13}CH_3$ (see Tables S1 and S2 in the Supporting Information).

Typically, for small values of the J quantum number, different nuclear spins within a given molecule can couple with each other via the so-called **I·I** interaction, where **I** is the nuclear spin (with corresponding quantum number I). The nuclear spins can also couple to the molecule's rotational motion, giving rise to the so-called **I·J** nuclear spin−rotation interaction.[36] In addition, if a nucleus has a quadrupole moment (i.e., when $I \geq 1$), an interaction with the electric field gradient arising from the molecule's electron cloud can occur. Each of these interactions can produce small "hyperfine" splittings within the symmetric-top K components. Figures 2 and 3 show spectra measured with the FTMW instrument in which such hyperfine splittings were resolved, providing additional evidence for the presence of $HZnCH_3$.

Figure 2 shows the FTMW spectrum of the $J = 1 \rightarrow 0$ transition from the main isotopologue, $H^{64}ZnCH_3$. The large doublet feature (~80 kHz wide) arises from the Doppler effect in the expansion from the pulsed nozzle, which is characteristic of these experiments. The Doppler doublets are indicated on the spectrum by brackets. The resolution in these data is sufficiently high to discern a small splitting of ~10 kHz arising from the **I·I** coupling of the methyl group hydrogens, which generates a "shoulder" to the right of the main emission feature. The two hyperfine lines are indicated by F, the quantum number for the total angular momentum $\mathbf{F} = \mathbf{I} + \mathbf{J}$. This hyperfine splitting was measured only for the $H^{64}ZnCH_3$ and $H^{66}ZnCH_3$ isotopologues.

Figure 3 presents a spectrum of the $J = 2 \rightarrow 1$ rotational transition of $H^{67}ZnCH_3$ that shows a section of the hyperfine pattern arising from the quadrupole moment of the ^{67}Zn nucleus ($I = 5/2$), the only isotope studied that has a nuclear spin $I \geq 1$.

(35) Townes, C. H.; Schawlow, A. L. *Microwave Spectroscopy*; Dover Publications: Mineola, NY, 1975.
(36) Hirota, E. *Springer Ser. Chem. Phys.* **1985**, *40*, 33–47.

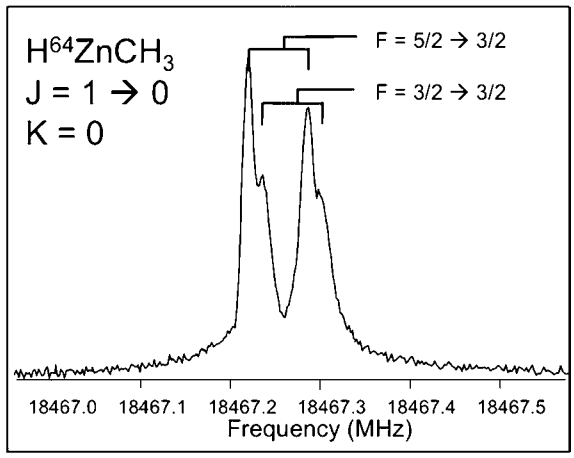

Figure 2. Spectrum of the $J = 1 \rightarrow 0$ transition of $H^{64}ZnCH_3$, measured with the FTMW system near 18 GHz, showing two hyperfine components, $F = {}^5/_2 \rightarrow {}^3/_2$ and ${}^3/_2 \rightarrow {}^3/_2$, arising from the $\mathbf{I}\cdot\mathbf{I}$ interaction of the methyl hydrogen nuclei ($I_{tot} = {}^3/_2$). The Doppler doublets, present for each component, are indicated by brackets. The spectrum is 600 kHz wide and was acquired from 5000 averaged pulses.

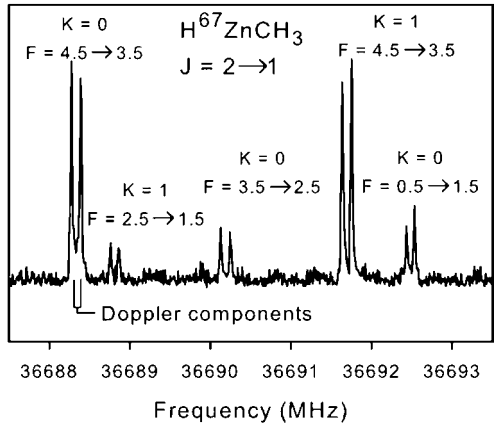

Figure 3. Spectrum of a portion of the $J = 2 \rightarrow 1$ rotational transition of $H^{67}ZnCH_3$, measured with the FTMW instrument near 37 GHz, showing part of the ^{67}Zn hyperfine structure in the $K = 0$ and $K = 1$ components. Each feature, labeled by the quantum numbers K and F, is split into Doppler doublets, as indicated in the figure. In this case, the hyperfine splitting far exceeds that of the Doppler components. This spectrum is a composite of 30 scans, each of which was 200 kHz wide and acquired from 5000 pulses.

(There is a much smaller contribution from the nuclear spin−rotation coupling as well.) Here the quadrupole coupling significantly alters the expected pattern. Each K component is split into several hyperfine features, labeled by the quantum number F. In this case, the hyperfine splitting is far larger than the splitting of the Doppler doublets. Other hyperfine components were measured outside of the frequency range shown in the figure, and those frequencies are available in Table S3 in the Supporting Information.

Multiple rotational transitions were measured for $HZnCH_3$ and its isotopologues. The complete data set is available in Tables S1−S3 in the Supporting Information. A subsection of the frequency measurements is presented in Table 1. Most of these data were obtained with the millimeter/submillimeter spectrometer. A total of 13 transitions ($J \leftrightarrow J + 1$) were recorded for $H^{64}ZnCH_3$, the main isotopic species; between four and six transitions were measured for the other six isotopologues $H^{66}ZnCH_3$, $H^{67}ZnCH_3$, $H^{68}ZnCH_3$, $D^{64}ZnCH_3$, $D^{66}ZnCH_3$, and $H^{64}Zn^{13}CH_3$ (see Tables S1−S3). For each transition, multiple K components were measured, typically $K = 0-6$ except in the case of the low-J transitions, for which only a few such components exist. In the case of $H^{67}ZnCH_3$, the transition frequencies of the ^{67}Zn hyperfine components were recorded for the lowest rotational lines ($J = 1 \rightarrow 0$ and $2 \rightarrow 1$), as shown in Table S3. A few hyperfine lines arising from the methyl protons were also resolved for $H^{66}ZnCH_3$ and $H^{64}ZnCH_3$, as discussed above (see Table S1).

Spectroscopic Analysis. The spectral transition frequencies for each of the seven isotopologues were fit to a molecular Hamiltonian. Rotational, centrifugal distortion, and in certain cases hyperfine constants were determined from this Hamiltonian using the nonlinear least-squares fitting routine SPFIT.[37] The data were weighted with respect to the experimental accuracy of the two different experimental techniques. In addition to the rotational constant B, the centrifugal distortion constants D_J, D_{JK}, H_{JK}, and H_{KJ} were necessary for a good fit. Hyperfine constants were also established for the appropriate isotopologues. For $H^{67}ZnCH_3$, both nuclear spin−rotation and quadrupole interactions were considered. The first term is described by a 3×3 tensor:[35]

$$E_{\mathbf{I}\cdot\mathbf{J}} = \sum_{\alpha,\beta} C_{\alpha\beta} I_\alpha J_\beta \tag{2}$$

The expression simplifies when the nuclear spin is on the C_{3v} axis, as is the case for $H^{67}ZnCH_3$, because only two constants, C_{aa} and C_{bb}, need to be considered in eq 2. The quadrupole interaction takes the form[35]

$$E_{eqQ} = \frac{eqQ\left[3\dfrac{K^2}{J(J+1)} - 1\right]}{2I(2I-1)(2J-1)(2J+3)} \times \left[\frac{3}{4}C(C+1) - I(I+1)J(J+1)\right] \tag{3}$$

where $C = F(F+1) - I(I+1) - J(J+1)$. This expression applies when the nucleus with the spin is on the C_{3v} axis, as in $H^{67}ZnCH_3$. The hyperfine splittings for $H^{64}ZnCH_3$ and $H^{66}ZnCH_3$ in the $K = 0$ lines arise from $\mathbf{I}_H\cdot\mathbf{I}_H$ coupling of the methyl hydrogens, which is quantified using the D_{HH} constant. These nuclei are equivalent, so their exchange must be considered when determining the total angular momentum quantum number F.[38] In the case of $K = 0$, $I_{tot}(H) = {}^3/_2$.[35]

The resulting molecular constants for each isotopologue are presented in Table 2. The root-mean-square deviations (rmsd) of the fits ranged from 16 to 41 kHz. It should be noted that the A rotational constant could not be determined because all of the recorded transitions were within a given K ladder (i.e., they had $\Delta K = 0$). The derived values of D_{HH} were 27−31 kHz, which are similar to value for CH_3CN (20.49 kHz).[38] The values of C_{aa} and C_{bb} were also very small (~6 kHz).

The bond lengths and bond angles of methylzinc hydride in the X^1A_1 electronic ground state were determined from the values of the rotational constant B for the seven isotopologues, recognizing that the species has C_{3v} symmetry. From the seven corresponding moments of inertia, I_b, a nonlinear least-squares analysis was performed using the STRFIT code in order to determine the r_0 structure.[39] This method is thought to be

(37) Pickett, H. M. *J. Mol. Spectrosc.* **1991**, *148*, 371–377.
(38) Kukolich, S. G.; Lind, G.; Barfield, M.; Faehl, L.; Marshall, J. L. *J. Am. Chem. Soc.* **1978**, *100*, 7155–7159.
(39) Kisiel, Z. *J. Mol. Spectrosc.* **2003**, *218*, 58–67.

Table 1. Selected Rotational Transition Frequencies (in MHz) for $HZnCH_3$ (X^1A_1)

			$H^{64}ZnCH_3$		$D^{64}ZnCH_3$		$H^{64}Zn^{13}CH_3$	
$J' \rightarrow J''$	K	$F' \rightarrow F''$	ν	$\Delta\nu^a$	ν	$\Delta\nu^a$	ν	$\Delta\nu^a$
1 → 0	0	$^5/_2 \rightarrow {}^3/_2$	18467.253	−0.003			17678.228	0.012
		$^3/_2 \rightarrow {}^3/_2$	18467.268	−0.001				
2 → 1	0	$^7/_2 \rightarrow {}^5/_2$	36934.272	−0.003			35356.197	−0.012
		$^3/_2 \rightarrow {}^1/_2$	36934.290	0.000				
	1		36933.348	0.001			35355.357	0.007
21 ← 20	0		387442.978	0.008	364150.363	0.025	370900.983	0.058
	1		387433.283	0.012	364141.267	0.040	370891.896	−0.009
	2		387404.184	0.004	364113.871	−0.024	370864.808	−0.034
	3		387355.712	−0.009	364068.315	−0.026	370819.693	−0.045
	4		387287.956	0.024	364004.543	−0.022		
	5		387200.894	0.027				
	6		387094.557	−0.039				
22 ← 21	0		405854.802	−0.009	381460.072	0.017	388527.904	0.003
	1		405844.657	0.002	381450.521	0.011	388518.421	−0.029
	2		405814.177	−0.019	381421.862	−0.014	388490.097	−0.002
	3		405763.452	−0.006	381374.155	0.002	388442.827	−0.020
	4		405692.477	−0.005				
	5		405601.322	−0.001				
	6		405490.049	−0.007				
	7		405358.763	−0.004				
23 ← 22	0				398765.478	0.000	406149.948	−0.048
	1				398755.484	−0.015	406140.113	−0.003
	2				398725.559	−0.005	406110.556	0.080
	3				398675.681	0.010	406061.113	0.037

[a] $\Delta\nu = \nu_{obsd} - \nu_{calcd}$.

Table 2. Spectroscopic Constants (in MHz) for Isotopologues of $HZnCH_3$ (X^1A_1)[a]

	$H^{64}ZnCH_3$	$H^{66}ZnCH_3$	$H^{67}ZnCH_3$	$H^{68}ZnCH_3$	$D^{64}ZnCH_3$	$D^{66}ZnCH_3$	$H^{64}Zn^{13}CH_3$
B	9233.6491(16)	9191.7064(23)	9171.5749(11)	9152.0759(51)	8677.4195(84)	8645.0423(77)	8839.1262(25)
D_J	0.0099960(14)	0.0099175(21)	0.0098807(38)	0.0098447(41)	0.0081331(80)	0.0080830(75)	0.0092424(29)
D_{JK}	0.23230(16)	0.22997(56)	0.22784(81)	0.22785(62)	0.21693(19)	0.21498(14)	0.21478(28)
H_{JK}	0.000001527(84)	0.00000159(48)		0.00000156(51)			
H_{KJ}	0.0000153(20)						
D_{HH}	0.027(25)	0.031(26)					
C_{aa}(Zn)			0.0065(16)				
C_{bb}(Zn)			0.0059(21)				
eqQ(Zn)			−109.115(31)				
rmsd of fit	0.020	0.016	0.031	0.025	0.025	0.041	0.035

[a] Values in parentheses are 3σ.

accurate to about ±0.005 Å. The r_0 computation assumes that each of the bond distances is the same for all of the isotopologues, which results in an error of a few percent because of the presence of zero-point vibrations. The H−Zn bond distance is the most sensitive to errors from the r_0 analysis because of the deuterium substitution. Uncertainties as large as 0.03 Å have been reported for heavy atom−hydrogen bond lengths.[40]

Discussion

Structure of $HZnCH_3$. The structure determined for methylzinc hydride in this study is shown in Figure 4 and summarized in Table 3. For comparison, the geometries of related molecules ($ZnCH_3$, ZnH, $HCuCH_3$, $CuCH_3$, and CH_4) are also included in the table. As the figure shows, the H−Zn−C backbone is linear. Any off-axis displacement of the terminal hydrogen would have broken the C_{3v} symmetry, lifting the K degeneracy and producing a spectrum characteristic of an asymmetric top. The observed H−Zn and Zn−C bond distances are 1.521 and 1.928 Å, respectively, while for the methyl group, the C−H bond distance is 1.140 Å and ∠HCH = 108.7°. Interestingly, Cd and Mg are also calculated to assume the same symmetric-top structure in their $HMCH_3$ analogues, while Pd and Ca are predicted to have bent backbones.[28]

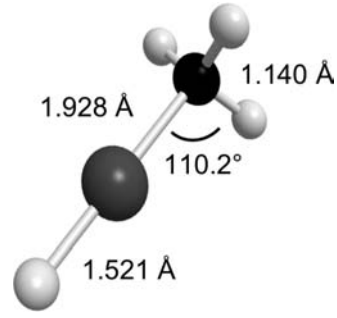

Figure 4. Experimental (r_0) structure of $HZnCH_3$, which exhibits clear C_{3v} symmetry with a H−Zn−C covalent bond on the symmetry axis.

This experimental geometry agrees fairly well with the r_e structures predicted by Alikhani[24] and de Jong et al.[28] (it should be noted that there can be significant differences between r_e

(40) Hollas, J. M. *High Resolution Spectroscopy*; Butterworths: London, 1982; p 138.

(41) Cerny, T. M.; Tan, X. Q.; Williamson, J. M.; Robles, E. S. J.; Ellis, A. M.; Miller, T. A. *J. Chem. Phys.* **1993**, *99*, 9376–9388.

(42) Tezcan, F. A.; Varberg, T. D.; Stroh, F.; Evenson, K. M. *J. Mol. Spectrosc.* **1997**, *185*, 290–295.

Table 3. Structures of $HZnCH_3$ and Similar Molecules

	r_{HM} (Å)	r_{MC} (Å)	r_{CH} (Å)	∠MCH (deg)	∠HCH (deg)	method	ref
$HZnCH_3$	1.5209(1)	1.9281(2)	1.140(9)	110.2(3)	108.7(3)	r_0	this work[a]
	1.532	1.937	1.092	110.9	108.0	r_e[b]	24
	1.533	1.954	1.098	110.7		r_e[c]	28
$ZnCH_3$		2.001(7)	1.105		109.21	r_0[d]	41
ZnH	1.6109					r_0	42
$HCuCH_3$	1.544	2.385	1.074	97.4		r_e[e]	26
$CuCH_3$		1.8841(2)	1.091(2)		110.07(8)	r_0[f]	45
CH_4			1.09403(1)		109.5	r_0	46

[a] Errors are 3σ based solely on the uncertainties in the rotational constants (see the text). [b] B3PW91. [c] ZORA-BLYP/TZ2P. [d] Errors are 1σ; r_{CH} and ∠HCH were held fixed. [e] SCF. [f] Errors are 1σ.

and r_0 structures.) Our gas-phase structure is also consistent with that found in the matrix studies of $HZnCH_3$.[20] However, our experimental r_0 H−Zn and Zn−C bond lengths are slightly shorter (by 0.01−0.02 Å) than the theoretical predictions, while the C−H bond distance is longer by ∼0.04 Å. Moreover, both the Zn−C and Zn−H bonds are 0.07−0.09 Å shorter than in the corresponding radical species, $ZnCH_3$ and ZnH.[41,42] The shortening of the H−Zn and Zn−CH_3 bonds relative to the corresponding open-shell fragments can be attributed to the stabilization gained by the addition of the axial hydrogen. An analogous result was observed for HZnCl and ZnCl, where the Zn−Cl bond is 0.05 Å shorter in HZnCl than in ZnCl.[43,44]

The methyl group parameters of $HZnCH_3$ can be compared with those of similar species. The C−H r_0 bond length in $HZnCH_3$ is ∼0.05 Å longer than that in CH_4 or $CuCH_3$.[45,46] Also, ∠HCH in $HZnCH_3$ is contracted by ∼1° relative to the value for those two species (see Table 3). Thus, it appears that the addition of a hydrogen atom distorts the methyl group, as is also theoretically predicted for $HCuCH_3$.[26] Unfortunately, the most interesting comparison of the methyl hydrogens ($HZnCH_3$ vs $ZnCH_3$) is not possible because the C−H bond length and ∠HCH were fixed in the structural analysis of $ZnCH_3$.[41]

Bonding in $HZnCH_3$. An intepretation of the bonding in methylzinc hydride can be derived from the ^{67}Zn nuclear quadrupole parameter, *eqQ*, which provides a measure of the electric field gradient across the zinc nucleus. A more symmetric charge distribution, as found in ionic species, leads to small absolute values of *eqQ*; the magnitude increases with the degree of covalent character.[35] The highly ionic molecule Zn^+F^- has an *eqQ* value of −60 MHz.[47] HZnCN has more covalent character, which is reflected in its quadrupole constant, $eqQ = -104.578(28)$ MHz.[34] In comparison, $eqQ = -109.125(11)$ for $HZnCH_3$. The quadrupole constant in ZnF is smaller in magnitude because the lone unpaired electron on the zinc nucleus resides in an orbital that is ∼90% Zn(4s) in character;[47] naturally, an s orbital produces a symmetric electric field. The larger magnitude of the *eqQ* value observed for $HZnCH_3$ indicates a larger covalent contribution to the bonding, likely arising from hybridization of the 4s and 4p orbitals on zinc, as suggested by Castillo et al.[25] Alikhani also concluded that all six atoms in $HZnCH_3$ form covalent, single bonds,[24] in agreement with this analysis.

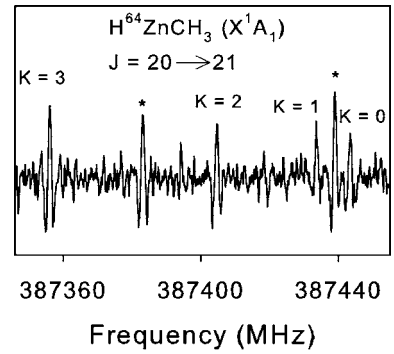

Figure 5. Observed rotational spectrum of the $J = 20 \rightarrow 21$ transition of $HZnCH_3$ created from a DC discharge of Zn(g) and CH_4 in Ar carrier gas. The $K = 0$, 1, 2, and 3 components are labeled, and two unidentified lines are marked with asterisks. This figure covers part of the frequency region shown in Figure 1. The spectrum is 110 MHz wide and signal-averaged over three scans, each acquired in 60 s.

Formation Mechanisms. It is well-known that zinc in its excited 4s4p state can insert into C−H and H−H bonds.[7] It is therefore quite possible that Zn atoms insert directly into C−H bonds to form $HZnCH_3$ during the gas-phase reaction of Zn vapor + CH_4. $HZnCH_3$ is unmistakably produced in the X^1A_1 state in the reaction chamber in the presence of Zn atoms, CH_4, and an electric discharge. The electrical discharge could be responsible for exciting the zinc atoms directly or through collisions with metastable argon atoms. A spectrum observed under these conditions is shown in Figure 5. Here, the $K = 0$, 1, 2, and 3 components of the $J = 20 \rightarrow 21$ rotational transition clearly show the presence of $HZnCH_3$, although the signals are somewhat weaker than those originating with the precursor $Zn(CH_3)_2$ (see Figure 1).

A large number of processes could occur in the discharge, however. One possible mechanism for methylzinc hydride formation is given by reaction R1:

$$Zn + CH_4 \xrightarrow{Ar} ZnCH_3 + H \xrightarrow{Ar} HZnCH_3 \qquad (R1)$$

Here $ZnCH_3$ is first created from neutral zinc atoms and methane, as observed for $CuCH_3$,[45] and then undergoes hydrogen addition to form $HZnCH_3$. However, this mechanism can reasonably be ruled out becaue there was no evidence of $ZnCH_3$ in the observed spectra.

Alternatively, ZnH may be formed first and then proceed to $HZnCH_3$ (reaction R2):

$$Zn + CH_4 \xrightarrow{Ar} ZnH + CH_3 \xrightarrow{Ar} HZnCH_3 \qquad (R2)$$

(43) Pulliam, R. L.; Sun, M.; Flory, M. A.; Ziurys, L. M. *J. Mol. Spectrosc.* **2009**, *257*, 128–132.
(44) Tenenbaum, E. D.; Flory, M. A.; Pulliam, R.; Ziurys, L. M. *J. Mol. Spectrosc.* **2007**, *244*, 153–159.
(45) Grotjahn, D. B.; Halfen, D. T.; Ziurys, L. M.; Cooksy, A. L. *J. Am. Chem. Soc.* **2004**, *126*, 12621–12627.
(46) Duncan, J. L. *J. Mol. Struct.* **1974**, *22*, 225–235.
(47) Flory, M. A.; McLamarrah, S. K.; Ziurys, L. M. *J. Chem. Phys.* **2006**, *125*, 194304.

Although weak ZnH signals were found in the spectral data, it is a thermodynamically stable dissociation product of $HZnCH_3$,[24] making this pathway improbable.

As suggested above, another possible source of $HZnCH_3$ is the direct insertion of zinc atoms into methane (reaction R3):

$$Zn + CH_4 \xrightarrow{Ar} HZnCH_3 \qquad (R3)$$

The insertion reaction of atomic zinc into CH_4 has been known to occur in solid matrices at low temperatures, where the matrix cage stabilizes $HZnCH_3$, the product of the reaction.[12] However, theoretical calculations disagree on the formation of this molecule in the gas phase. Calculations by Alikhani suggested that the gas-phase reaction of Zn and CH_4 leads to the formation of $HZnCH_3$ in the excited $^3A'$ state, which immediately decomposes into ZnH and CH_3.[24] The $^3A'$ state is created when the insertion occurs through the Zn(4s4p ^{3}P) excited state. Other calculations have suggested that the gas-phase reaction between the Zn(^{1}P) excited state with methane would yield $HZnCH_3$ in the $^1A_1$ ground state; this is a stable intermediate lying 21.2 kcal/mol in energy above Zn(^{1}S) and CH_4.[25] Unfortunately, the DC discharge is not a selective excitation method, so it is possible that both the ^{1}P and ^{3}P states of zinc are present, either of which may be responsible for the proposed insertion mechanism. The presence of a third body, namely, Ar, may help in the stabilization of $HZnCH_3$. On the basis of our experimental results, it is possible that zinc atoms can activate C−H bonds in methane in the gas phase under certain conditions.

Conclusions

An unusual 3d transition-metal species, $HZnCH_3$, has been characterized in the gas phase using rotational spectroscopy. This is the first experimental study to establish the detailed structure of an insertion product of a metal atom into methane. The species has a $^1A_1$ ground electronic state with C_{3v} symmetry. The structure determined in this work shows that addition of the hydrogen atom stabilizes the molecule, although it also creates a slight distortion of the methyl group. The electric quadrupole moment determined for $H^{67}ZnCH_3$ suggests covalent bonding at the zinc nucleus, consistent with theoretical predictions. Synthetic tests indicate that $HZnCH_3$ can be created from the gas-phase reaction of Zn atoms and CH_4, perhaps by the insertion of excited metal atoms into the C−H bond. Studies of additional methylmetal hydride compounds in the gas phase would further test metal reactivity as well as establish whether any unusual geometries with bent backbones exist.

Acknowledgment. This work was supported by NSF Grant CHE-07-18699.

Supporting Information Available: Tables of observed rotational transitions of the seven isotopologues studied. This material is available free of charge via the Internet at http://pubs.acs.org.

JA106121V